Research Article

Journal of Environmental Nanotechnology

Tunable Electrochemical Properties of Cobalt-doped Praseodymium Oxide Perovskite *via* Sol-gel Synthesis for Supercapacitor Applications

A. Cathirin Preethi[1], V. Hariharakrishnan[1], V. Saraswathi[1*], D. Saravanan[2] and S. Meiyazhagan[3]

[1]PG and Research Department of Physics, National College (Affiliated to Bharathidasan University), Tiruchirappalli, TN, India
[2]Department of Chemistry, National College (Affiliated to Bharathidasan University), Tiruchirappalli, TN, India
[3]Department of Science and Humanities (Physics), Karpagam College of Engineering (Affiliated to Anna University), Coimbatore, TN, India
Received: 30.06.2025 Accepted: 06.08.2025 Published: 30.09.2025
*saraswathiv@nct.ac.in

ABSTRACT

Cobalt-doped praseodymium oxide ($Pr_{1-x}Co_xO_3$) perovskite was successfully synthesized *via* the sol-gel method for enhanced electrochemical performance as supercapacitor electrodes. The doping strategy enabled precise control over the nanostructure, achieving an average particle size of approximately 20.65 nm with spherical, agglomerated morphology, as revealed by scanning electron microscopy. Energy-dispersive X-ray spectroscopy confirmed a uniform elemental distribution throughout the material. Brunauer–Emmett–Teller analysis showed a notable increase in surface area to 9.297 m^2/g and a decreased pore volume of 0.062 cc/g compared to undoped Pr oxide, facilitating improved electrolyte diffusion and charge transport. Fourier-transform infrared spectrum exhibited characteristic metal–oxygen vibrational bands at 1554.82, 1410.10, and 657.96 cm^{-1}, confirming the perovskite structure. X-ray photoelectron spectroscopy further validated the chemical states, identifying Pr^{3+} peaks at 933.84 and 944.04 eV, oxygen vacancies *via* O 1s peaks at 528.6 and 531.2 eV, and mixed Co^{2+} /Co^{3+} oxidation states through Co 2p peaks at ~780.1 and ~795.3 eV with satellite features. Electrochemical studies revealed a significant enhancement in specific capacitance, with the Co-doped material achieving 599 F/g at 3 A/g, substantially higher than the 270 F/g obtained for the undoped sample at 1 A/g. Furthermore, the electrode exhibited a high energy density of 27.5 Wh/kg and a power density of 4.9 kW/kg. These results demonstrate that cobalt incorporation effectively enhances charge storage capabilities, establishing $Pr_{1-x}Co_xO_3$ perovskite as a highly promising candidate for next-generation supercapacitor applications.

Keywords: Cobalt-doped praseodymium oxide; Sol-gel; Cyclic voltammetry; Electrochemical impedance spectroscopy; Energy storage materials.

1. INTRODUCTION

The growing demand for efficient and sustainable energy storage systems has spurred significant interest in developing advanced materials for supercapacitors and batteries. Supercapacitors are well-regarded for their high power density, rapid charge-discharge cycles, and long-term cycling stability (Naeem *et al.* 2023a; Pardeshi *et al.* 2024; Ejaz *et al.* 2024; Saha *et al.* 2024; Olabi *et al.* 2022). However, their relatively low energy density limits their broader application. In contrast, lithium-ion batteries offer high energy density but are hindered by slower charge rates and limited cycle life. To bridge this performance gap, recent efforts have focused on hybrid materials that integrate the advantages of both technologies, enabling enhanced power and energy densities for future generation storage systems (Yadlapalli *et al.* 2022; Lakshmi and Vedhanarayanan, 2023; Naeem, 2024a; Naeem *et al.* 2023b).

Among the various electrode materials investigated, transition metal oxides, particularly cobalt oxide (Co_3O_4), have attracted attention due to their high theoretical capacitance, favorable redox behavior, and moderate electrical conductivity. Nonetheless, cobalt oxide suffers from drawbacks such as poor cycling stability, low intrinsic conductivity, and limited charge storage efficiency, which challenge its practical deployment in supercapacitor devices (Naeem *et al.* 2024b; Jiang *et al.* 2024; Wei *et al.* 2024; Xu *et al.* 2024; Gao *et al.* 2025). To address these issues, doping strategies using rare-earth elements have emerged as a viable route to tune the physicochemical and electrochemical properties of metal oxides. Rare-earth doping can introduce oxygen vacancies, enhance electronic conductivity, and modulate the local electronic structure, thereby improving overall electrochemical performance (Tian *et al.* 2024; Alenad *et al.* 2023; Althubiti *et al.* 2023; Seliem *et al.* 2024a; Aman *et al.* 2023).

In this context, cobalt, a transition metal with notable redox activity, serves as an effective dopant in praseodymium-based oxides. Praseodymium, a rare-earth element, acts as the parent material, offering a stable oxide framework with unique electronic and structural properties. The incorporation of cobalt into the Pr-based lattice introduces additional oxygen vacancies, enhances electronic conductivity, and facilitates ion diffusion, thereby improving the redox performance and cycling stability of the material. (Gao and Wang, 2024; Lakal *et al.* 2022; Lokhande *et al.* 2024). While perovskite oxides such as lanthanum cobalt oxide ($LaCoO_3$) (Moorthi *et al.* 2024) and cerium-doped Co_3O_4 (Ali *et al.* 2020) have been extensively studied, less attention has been paid to cobalt doping into rare-earth-based oxides such as praseodymium oxide In particular, the structural and electrochemical behavior of cobalt-doped praseodymium perovskites ($Pr_{1-x}Co_xO_3$) remains largely unexplored. This study addresses that gap by systematically evaluating the structural and electrochemical properties of cobalt-doped praseodymium oxide, thereby introducing a novel and underexplored material system for supercapacitor applications.

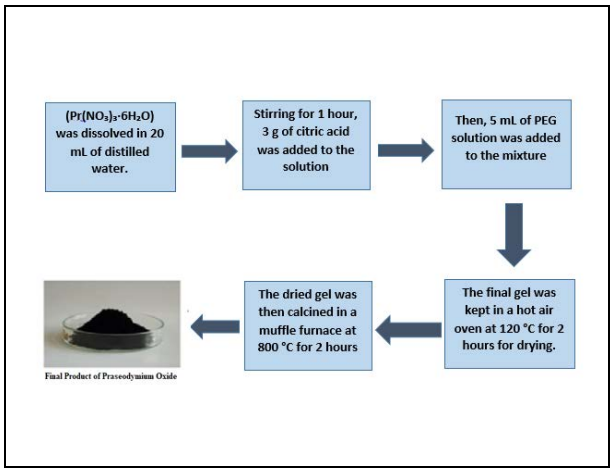


Fig. 1: Synthesis process of pure praseodymium oxide

Perovskite materials are known for their high ionic and electronic conductivity, structural robustness, and flexible compositional tunability *via* A- and B-site substitutions. These characteristics enable them to support rapid charge transfer and diffusion kinetics, critical for high-performance supercapacitors (Naeem, 2024c; Naeem *et al.* 2023c). By carefully selecting a substitution level of x = 0.2, the composition $Pr_{1-x}Co_xO_3$ was optimized to enhance redox activity without compromising structural stability. Excessive cobalt content could lead to phase segregation and reduced conductivity, whereas insufficient doping may not yield significant performance improvements. Literature reports suggest that ~20% substitution achieves a favorable balance between electrochemical activity and structural integrity.

In this work, a novel $Pr_{1-x}Co_xO_3$ perovskite was synthesized *via* a sol-gel route, enabling precise control over crystallinity, particle size and elemental dispersion. Compared to conventional hydrothermal or solid-state methods, the sol-gel process ensures improved material homogeneity and electrochemical performance.

This study presents the first comprehensive evaluation of cobalt-doped praseodymium oxide ($Pr_{1-x}Co_xO_3$) perovskites for supercapacitor applications. The novelty lies in the strategic use of cobalt substitution in a praseodymium-based perovskite matrix, an area previously underexplored in the context of energy storage.

2. MATERIALS AND METHODS

2.1 Synthesis of Pure Praseodymium Oxide (Pr_6O_{11})

To synthesize pure praseodymium oxide (Pr_6O_{11}), 6.48 g of praseodymium nitrate hexahydrate ($Pr(NO_3)_3 \cdot 6H_2O$) was dissolved in 40 mL of deionized water under constant stirring to form a homogeneous solution. Then, 3 g of citric acid (as a complexing agent) and 5 mL of polyethylene glycol (PEG, as a polymerizing and structure-directing agent) were added to the solution. The mixture was heated at 80–90°C to promote evaporation, leading to the formation of a viscous sol, which gradually transitioned into a gel. The obtained gel was dried at 120°C for 2 hours in a hot air oven to eliminate residual moisture. The dried product was then ground into a fine powder and calcined at 800°C for 3 hours in air with a heating rate of 5°C/min to ensure complete crystallization. After cooling to room temperature, the calcined material was reground to obtain pure praseodymium oxide powder (Fig. 1).

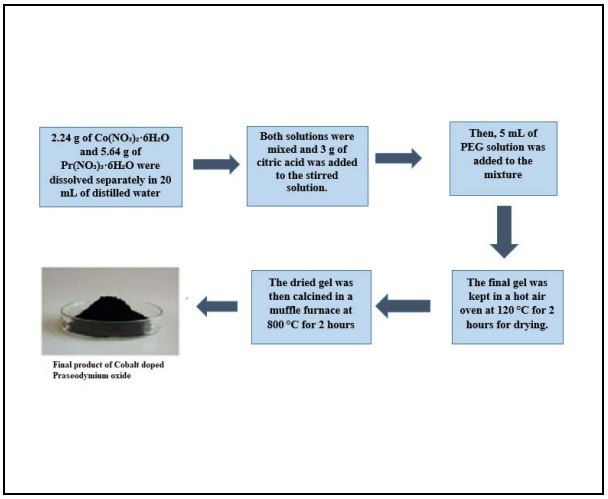


Fig. 2: Synthesis process of cobalt-doped praseodymium oxide

2.2 Synthesis of Cobalt-doped Praseodymium Oxide

For the preparation of cobalt-doped praseodymium oxide, 1.46 g of cobalt nitrate hexahydrate ($Co(NO_3)_2 \cdot 6H_2O$) was dissolved in 10 mL of deionized water and stirred to form a uniform cobalt solution. Separately, 8.78 g of praseodymium nitrate hexahydrate ($Pr(NO_3)_3 \cdot 6H_2O$) was dissolved in 20 mL of deionized water to prepare the praseodymium solution. The praseodymium solution was then slowly added to the cobalt solution with continuous stirring to ensure a well-mixed precursor solution. Subsequently, 3 g of citric acid and 5 mL of PEG were added to the mixture. The solution was heated at 80–90°C to evaporate the water content, resulting in a thick sol that eventually formed a gel. The gel was then dried at 120°C for 2 hours to remove any remaining water.

The dried gel was calcined at 800°C for 3 hours in an air atmosphere using a ramp rate of 5°C/min to ensure uniform phase development and crystallinity. The cooled product was then ground to obtain fine Pr1-xCoxO3 powder. The final product is a homogeneous $Pr_{1-x}Co_xO_3$ perovskite material (Fig. 2), which was characterized by X-ray diffraction (XRD) to analyze its crystalline phase, scanning electron microscopy (SEM) for morphology, and energy-dispersive X-ray spectroscopy (EDX) and XPS to verify the dopant distribution and elemental composition.

3. RESULTS AND DISCUSSION

3.1 X-ray Diffraction

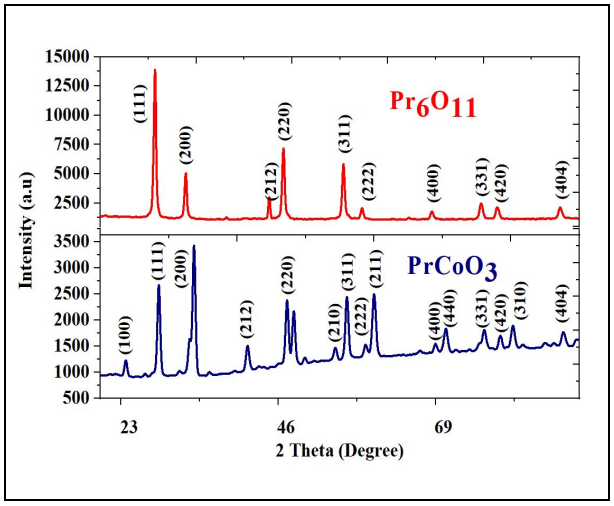


Fig. 3: XRD patterns of pure praseodymium oxide and Cobalt doped praseodymium oxide

The XRD patterns of the samples were examined using a Powder X-Ray Diffractometer (X' Pert Pro - PAnalytic). Fig. 3 compares the crystalline structures of Pr_6O_{11} and $PrCoO_3$, highlighting the difference in their phase composition and crystallinity. The diffraction peaks correspond to different crystallographic planes, indexed with Miller indices. Pr_6O_{11} exhibits a cubic structure, space group Fm3m (225) (JCPDS Card 00-042-1121) (Matović *et al.* 2013), while $PrCoO_3$ adopts a cubic perovskite structure, space group Pm-3m (221) (JCPDS CARD- 01-075-0280). The variation in peak intensity and positions between these two materials indicates distinct crystallographic arrangements, suggesting differences in lattice parameters and atomic positioning. The ionic radii of Pr^{3+} and Co^{3+} play a crucial role in stabilizing these structures. Praseodymium in Pr_6O_{11} exists in mixed oxidation states (Pr^{3+}/Pr^{4+}), leading to oxygen vacancy formation, which affects the material's electrical and catalytic properties. On the other hand, in $PrCoO_3$, cobalt exists in a low-spin Co^{3+} state, with praseodymium acting as a stabilizing A-site cation, influencing the overall lattice distortion due to ionic size mismatch. The ionic radius of Pr^{3+} (~1.13 Å) is relatively larger than that of Co^{3+} (~0.545 Å), significantly impacting the bond angles and bond lengths within the perovskite framework (Naeem *et al.* 2023d).

The calculated crystallite sizes of Pr_6O_{11} (27.28 nm) and $PrCoO_3$ (20.65 nm), obtained using the Debye-Scherrer formula, highlight their structural differences. The formula used is:

$$D = k\lambda/\beta cos\theta \quad \ldots (1)$$

where

D is the crystallite size,

K is the shape factor (typically 0.9),

λ is the X-ray wavelength (1.5406 Å for Cu Kα radiation),

β is the full width at half maximum (FWHM) of the diffraction peak (in radians), and

θ is the Bragg angle.

The larger crystallite size of Pr_6O_{11} suggests better crystallinity with fewer grain boundaries, enhancing its thermal and electrical stability, making it ideal for solid oxide fuel cells (SOFCs) and oxygen transport membranes. The smaller crystallite size of $PrCoO_3$ increases surface area, which is beneficial for catalytic applications like oxygen reduction and oxidation reactions. This variation in crystallite size, along with ionic radii and oxidation states, directly impacts their functional properties, making them suitable for energy and electronic applications (Zeshan *et al.* 2024; Zahra *et al.* 2024a).

Table 1. Measured crystallite size from XRD analysis and comparison of XRD spectra with standard JCPDS cards

Sample	Phase Identified	Crystallite Size (nm)	Major Peak Positions (2θ, Degrees)	Crystal Structure	JCPDS Card Number
Pure Pr (Pr_6O_{11})	Praseodymium Oxide (Pr_6O_{11})	27.28 nm	28.5°, 33.2°, 47.5°, 56.3°	Cubic (Fm3m)	00-042-1121
$Pr_{1-x}Co_xO_3$ (where x = 0.2)	Cobalt doped Praseodymium Oxide ($PrCoO_3$)	20.65 nm	23.6°, 32.4°, 46.8°, 58.7°	Cubic Perovskite (Pm-3m)	01-075-0280

3.2 Scanning Electron Microscopy

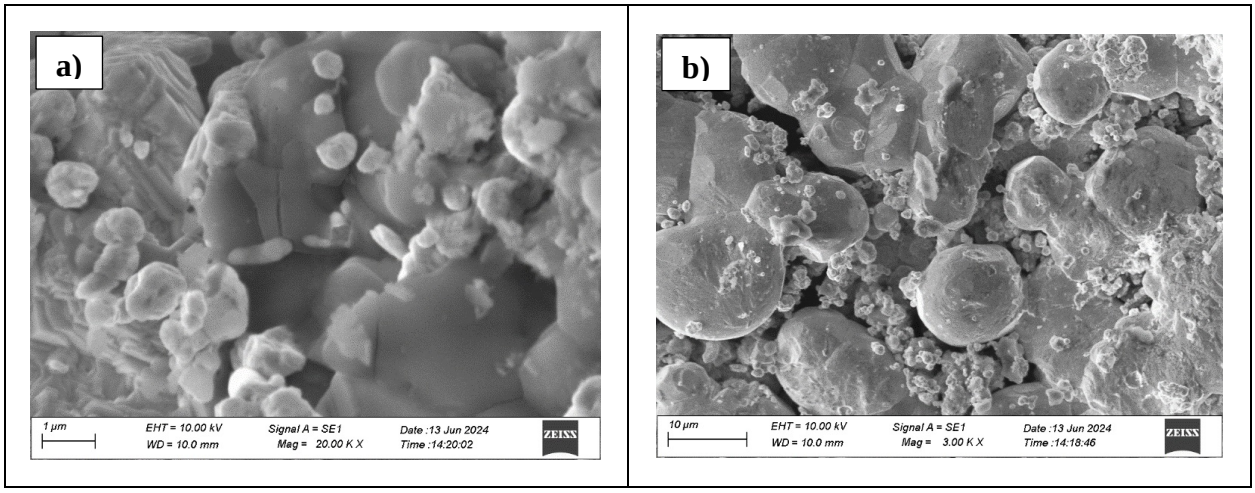


Fig. 4: (a) Morphological analysis of pure praseodymium oxide, (b) cobalt-doped praseodymium oxide

The SEM images were recorded on a SEM instrument with EDX (TESCAN OXFORD VEGA-3, INCA). They reveal the morphological differences between pure praseodymium oxide (Fig. 4a) and cobalt-doped praseodymium oxide (Fig. 4b) samples at varying magnifications. The pure Pr_6O_{11} sample displays fine, irregularly shaped particles with relatively smaller sizes, indicating a compact and dense morphology. These particles are slightly uniform in shape, suggesting that the crystallization process produces irregular structures with fine granularity. The Cobalt doped praseodymium oxide, shows significantly larger spherical particles that are agglomerated compared to the pure Pr_6O_{11} sample.

The role of ionic radii is key to understanding these changes. Praseodymium ion (Pr^{3+}) has a significantly larger ionic radius (~1.13 Å in eight-fold coordination) compared to cobalt (Co^{3+}, ~0.545 Å in six-fold coordination) (De *et al.* 2024). When Co is introduced into the Pr lattice, it alters the lattice parameters, inducing structural distortions that affect particle growth and agglomeration behavior. The larger Pr ions modify the crystallization dynamics, potentially leading to the formation of oxygen vacancies and changes in the electronic structure, which can enhance the material's electrochemical properties (Mahato *et al.* 2023; Manzoor *et al.* 2023). The observed change in morphology, characterized by larger, spherical, and more agglomerated particles, suggests that co doping promotes enhanced particle growth and aggregation. Pure Pr_6O_{11} particles exhibit a small size range of approximately 28 nm, with an irregular and fine-grained morphology. In contrast, cobalt-doped praseodymium oxide particles are significantly larger (~78 nm), forming spherical and agglomerated structures that enhance surface area and charge transport.

Table 2. Morphology analysis of particles

Sample	Particle Size (nm)	Shape	Observation
Pure praseodymium oxide	Small (~28nm)	Irregular, fine-grained	Compact and dense morphology with slightly uniform structures.
Cobalt-doped praseodymium oxide	Larger (~78 nm)	Spherical, agglomerated	Co doping promotes particle growth and aggregation, enhancing surface area and charge transport.

These modifications can improve critical characteristics such as surface area, conductivity, and porosity, which are essential for applications in energy

storage devices like supercapacitors. Therefore, the observed differences in particle size and shape between the pure- and Co-doped praseodymium oxide samples highlight the potential of Co doping to optimize crystallization behavior, ultimately improving electrochemical performance and catalytic activity for energy storage applications.

3.3 EDX Analysis of Pr oxide and Co-doped Pr oxide

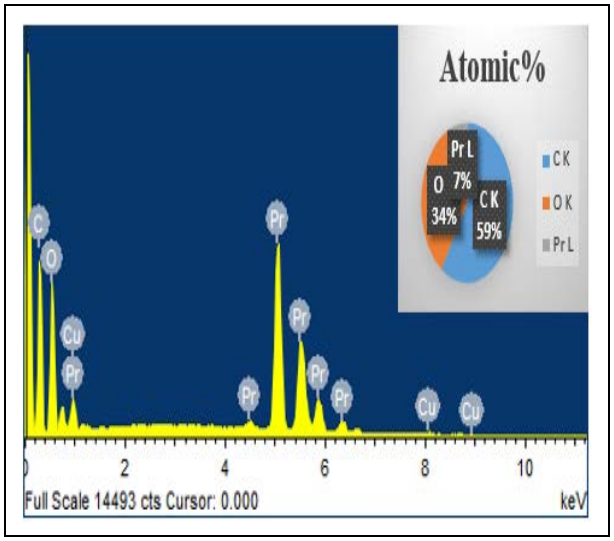


Fig. 5(a): EDX for pure praseodymium nanoparticles

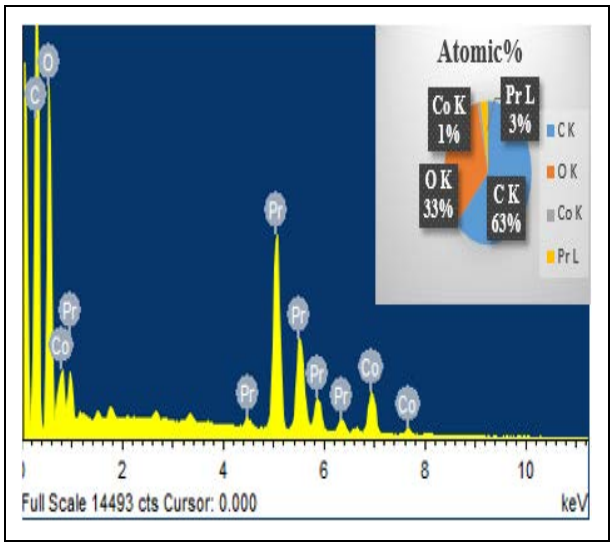


Fig. 5(b): EDX of cobalt doped praseodymium oxide nanoparticles

The Energy Dispersive X-ray Spectroscopy analysis of the pure and Co-doped praseodymium oxide samples reveals distinct compositional differences and elemental distributions. The EDX spectrum for pure Pr_6O_{11} (Fig. 5a) shows characteristic peaks corresponding to praseodymium (Pr), oxygen (O), carbon (C), and trace amounts of copper (Cu), with atomic percentages of 7% Pr-L, 34% O-K, and 59% C-K. The prominent Pr peaks at various energy levels indicate the successful synthesis of the praseodymium-based material, while the oxygen content suggests the formation of oxide phases. In comparison, the cobalt-doped praseodymium oxide sample (Fig. 5b) exhibits additional peaks corresponding to cobalt (Co), with a modified elemental distribution showing 3% Pr-L, 33% O-K, 63% C-K, and 1% Co-K. The appearance of Co peaks and their relative intensities confirms the successful incorporation of cobalt into the praseodymium matrix. Both spectra share similar peak positions for Pr, indicating that the basic crystal structure is maintained after Co doping, but with notable changes in peak intensities reflecting the modified elemental composition. The high carbon content in both samples likely originates from the carbon substrate used for EDX analysis or the carbon-based components in the synthesis process (Zahra *et al.* 2024b; Hussain *et al.* 2024a). The presence of trace Cu peaks in both spectra might be attributed to the sample holder or instrumental background. The consistent oxygen content around 33-34% in both samples suggests similar oxidation states and oxygen coordination environments. The relatively low atomic percentage of Co in the doped sample aligns with the intended dopant concentration, demonstrating precise control over the material's composition during synthesis. These compositional characteristics play a crucial role in determining the electrochemical properties and performance of these materials in supercapacitor applications.

Table 3. Elemental composition from EDX analysis

Element	Pure Pr_6O_{11} (% Atomic composition)	Cobalt-doped praseodymium oxide (%Atomic composition)
Pr (Praseodymium)	7%	3%
Co (Cobalt)	0%	1%
O (Oxygen)	34%	33%
C (Carbon)	59%	63%

3.4 Fourier Transmission Infrared Spectroscopy

Fourier-transform infrared spectrum was recorded in Bruker Alpha spectrophotometer in 4000–400 cm^{-1} frequency region.

The provided FTIR spectra illustrate the vibrational analysis of Pr_6O_{11} and $Pr_{1-x}Co_xO_3$ (Fig. 6), showing their characteristic absorption peaks. The broad absorption bands around 3433.94 cm^{-1} and 3429.51 cm^{-1} in both samples correspond to the stretching vibrations of O-H groups, indicating moisture or hydroxyl groups. The peaks observed around 2961–2928 cm^{-1} are attributed to C-H stretching vibrations, likely due to residual organic compounds from synthesis. In

Pr_6O_{11}, the peaks at 1549.39 cm^{-1} and 1466.85 cm^{-1} correspond to stretching vibrations of metal-oxygen bonds, while the fingerprint region below 1100 cm^{-1} exhibits characteristic metal-oxygen vibrations, particularly at 1077.30 cm^{-1}, 845.34 cm^{-1}, and 672.47 cm^{-1}. In $Pr_{1-x}Co_xO_3$ (where x = 0.2), strong absorption bands at 1554.82 cm^{-1} and 1410.10 cm^{-1} also confirm the presence of metal-oxygen interactions. The peaks at 1085.74 cm^{-1}, 841.69 cm^{-1}, and 657.96 cm^{-1} suggest Co-O and Pr-O vibrational modes, confirming the perovskite structure. Comparing both spectra, $Pr_{1-x}Co_xO_3$ exhibits better-resolved vibrational peaks in the low-wavenumber region, particularly in the metal-oxygen stretching region, making it superior for vibrational analysis. The sharper and more distinct peaks in $Pr_{1-x}Co_xO_3$ indicate well-defined bonding structures, making it more suitable for precise structural characterization (BaQais *et al.* 2023).

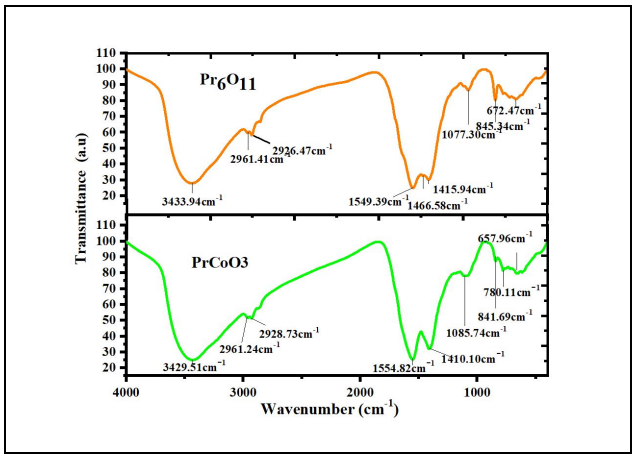


Fig. 6: FTIR analysis of pure Pr_6O_{11} and cobalt-doped praseodymium oxide

3.5. BET Analysis

Brunauer-Emmett-Teller (BET) analysis was recorded in BELSORP-maxII (BELSORP series) model and Microtrac BEL Corp: BELCONTROL software. The nitrogen adsorption–desorption isotherms reveal (Fig.7a and 7b) that pure praseodymium oxide exhibits mesoporous characteristics with a higher adsorbed volume, while cobalt-doped praseodymium oxide demonstrates a more uniform and well-developed porous structure. Interestingly, the specific surface area of cobalt-doped praseodymium oxide (9.297 m^2/g) is higher than that of the pure form (5.198 m^2/g), indicating that cobalt doping significantly alters the textural properties. This increase in surface area is attributed to structural rearrangements and the generation of oxygen vacancies caused by the incorporation of Co^{3+} ions, which also lead to lattice distortion (BaQais *et al.* 2023). These effects enhance ion diffusion, redox activity, and electrical conductivity. Additionally, the smaller crystallite size and reversible Co^{3+}/ Co^{2+} redox reactions contribute to improved charge storage, making cobalt-doped praseodymium oxide a more efficient material.

The pore volume of pure praseodymium oxide was measured at 0.122 cc/g, while that of cobalt-doped praseodymium oxide decreased to 0.062 cc/g (Fig. 8). This further confirms the structural modifications induced by doping. The pore size distribution analysis revealed that pure praseodymium oxide has a broader distribution with a peak at 800 nm, while cobalt-doped praseodymium oxide shows a sharper distribution with dominant pores below 50 nm, facilitating enhanced ion diffusion.

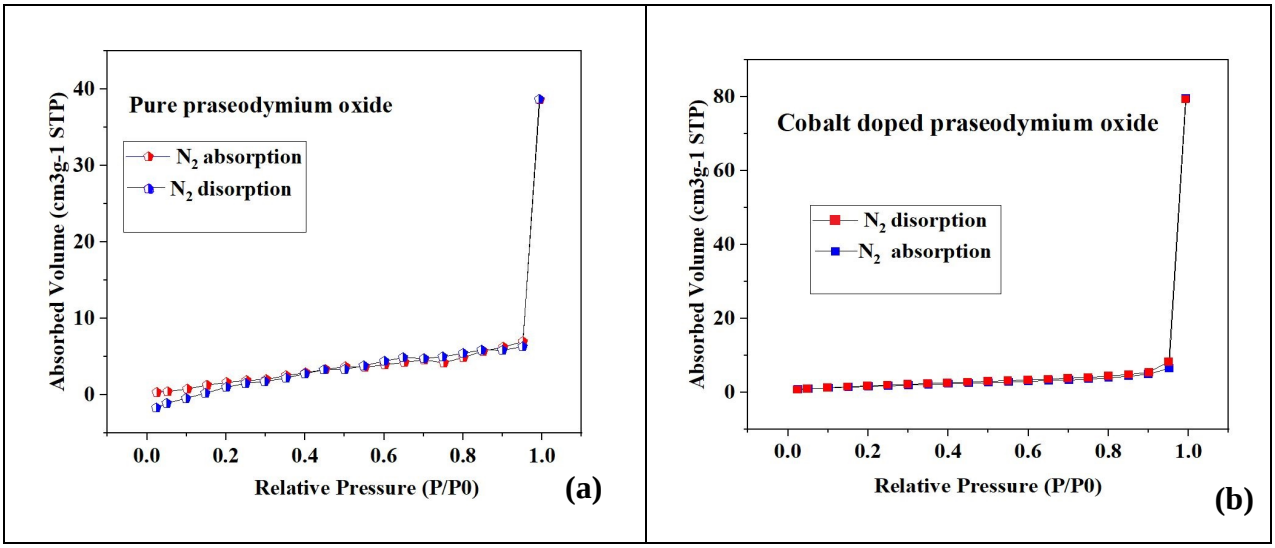


Fig. 7: BET analysis of (a) pure praseodymium oxide and (b) cobalt-doped praseodymium oxide

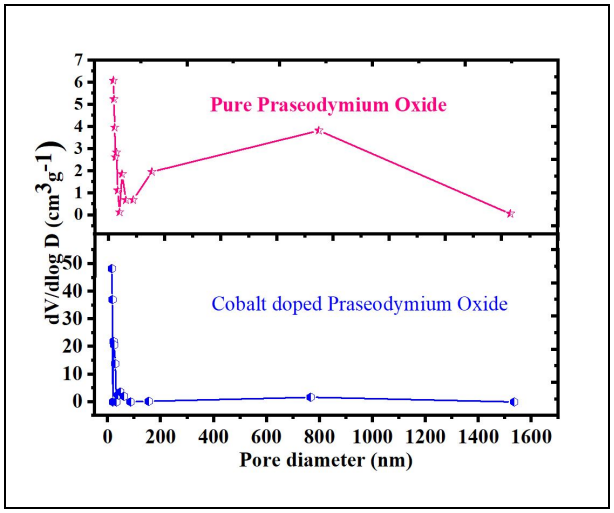


Fig. 8: Pore volume for pure Pr oxide and Co-doped Pr oxide

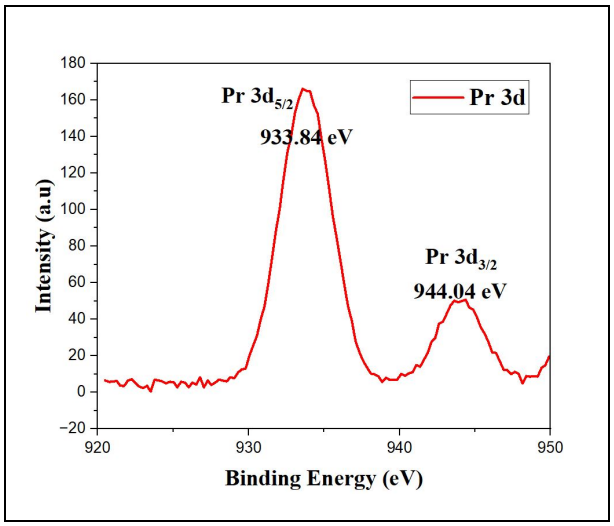


Fig. 9(a): XPS analysis of Pr

A well-balanced pore structure, as analyzed by BET, is essential for efficient charge storage in supercapacitors, as it enables rapid ion transport and minimizes resistance (Gouadria *et al.* 2025). The observed modifications in surface area and porosity suggest that cobalt doping can tune the electrochemical properties of praseodymium oxide, potentially enhancing its energy storage capabilities by improving charge transfer kinetics and ion accessibility.

3.6 XPS

The X-ray photoelectron spectroscopy analysis provides detailed insights into the elemental states and chemical environments of praseodymium oxide before and after cobalt doping. The Pr 3d spectrum shows (Fig. 9a) two prominent peaks at 933.84 eV (Pr $3d_{5/2}$) and 944.04 eV (Pr $3d_{3/2}$), which correspond to the spin-orbit doublet of Pr in the +3 oxidation state. These sharp and symmetric peaks indicate the presence of a stable praseodymium oxide phase with well-defined electronic structure and crystallinity.

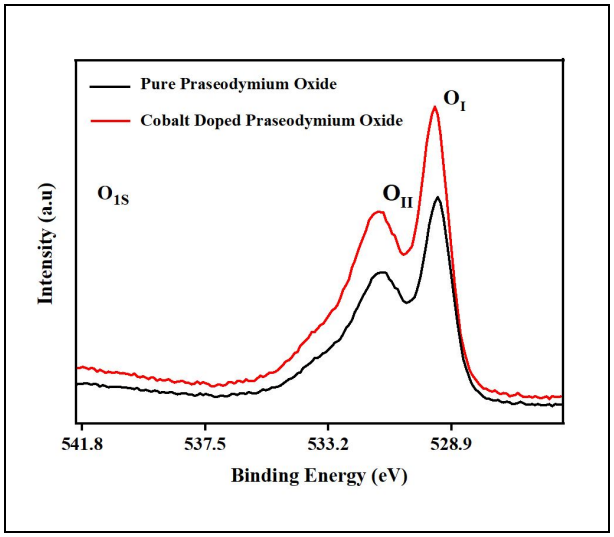


Fig. 9(b): XPS analysis of oxygen

The O 1s region (Fig. 9b) offers further confirmation of cobalt doping effects. In the spectrum, two distinct peaks are observed: OI (~528.5 eV), associated with lattice oxygen (O^{2-}), and OII (~531.5 eV), attributed to surface-adsorbed oxygen species or oxygen vacancies. A clear distinction is visible between pure praseodymium oxide (black line) and cobalt-doped praseodymium oxide, where the latter exhibits significantly higher intensity in the OII peak. This increase suggests a greater concentration of oxygen vacancies and surface defects induced by cobalt incorporation, which enhances the material's redox reactivity and surface chemistry.

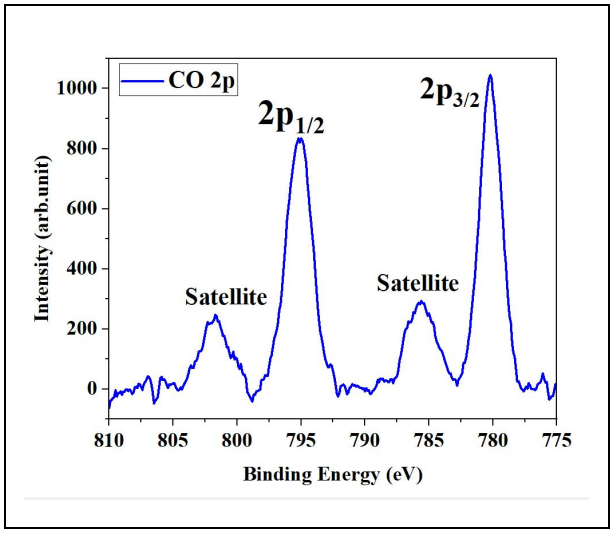


Fig. 9(c): XPS analysis of Cobalt

The Co 2p spectrum (Fig. 9c) confirms the successful doping of cobalt into the praseodymium oxide

matrix. It displays two main peaks at approximately 780 eV (Co $2p_{3/2}$) and 795 eV (Co $2p_{1/2}$), along with well-defined satellite peaks around 786 eV and 802 eV. These satellite features are characteristic of high-spin Co^{2+} and Co^{3+} states, indicating a mixed-valence environment typical of cobalt in oxide lattices such as CoO or Co_3O_4 (Alenad *et al.* 2023; Alshammari *et al.* 2024). The satellite structures result from shake-up transitions, affirming the presence of cobalt in a chemically active state. Cobalt doping introduces significant modifications to the praseodymium oxide structure. It leads to the formation of oxygen vacancies, alters the electronic environment, and enables potential Pr–O–Co interactions within the lattice. These changes contribute to enhanced electronic conductivity, increased surface reactivity, and improved electrochemical properties, making the doped material more suitable for energy storage or catalytic applications.

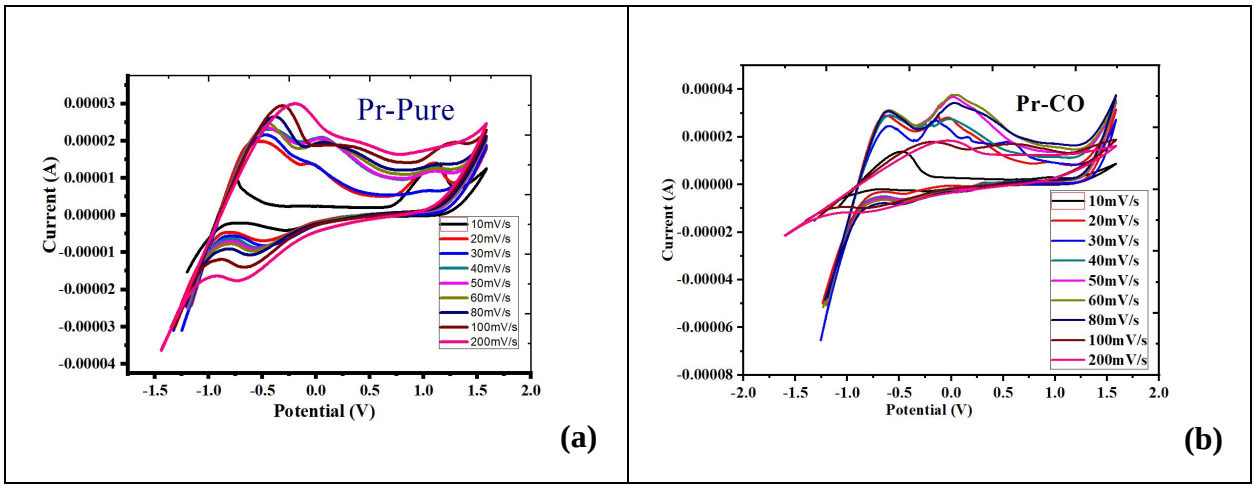


Fig. 10: (a) CV analysis of pure praseodymium oxide (b) cobalt-doped praseodymium oxide

3.7 Cyclic Voltammetry

The cyclic voltammetry (CV) analysis comparing pure praseodymium oxide (Fig. 10a) and cobalt-doped praseodymium oxide (Fig. 10b) samples reveals significant insights into their electrochemical performance for supercapacitor applications. Both samples were tested across various scan rates from 10 mV/s to 200 mV/s, showing distinct electrochemical behaviors. The pure praseodymium oxide sample exhibits quasi-rectangular CV curves with current responses ranging from -0.00003 to 0.00003 A within a potential window of -1.5 to 1.5 V, demonstrating typical double-layer capacitive behavior with some pseudocapacitive characteristics. In comparison, the cobalt-doped praseodymium oxide sample shows notably enhanced performance with higher current responses (approximately ±0.00004 A) and a wider potential window (-2.0 to 2.0 V vs Ag/AgCl), indicating improved charge storage capability. The specific capacitance, which can be calculated from the integrated area of the CV curves, appears significantly higher for the cobalt-doped praseodymium oxide sample due to its larger enclosed area. The CV curves of $PrCoO_3$ exhibit greater stability and consistency at higher scan rates, reflecting improved rate capability and quicker ion diffusion inside the electrode material.

The cobalt doping has effectively enhanced the electrochemical properties, as evidenced by the pronounced redox peaks and better curve symmetry in the cobalt-doped praseodymium oxide sample. These characteristics are particularly advantageous for supercapacitor applications, as they indicate improved energy storage capacity, better rate capability, and enhanced charge-discharge reversibility. The quasi-rectangular shape with distinct redox peaks suggests a beneficial combination of double-layer capacitance and pseudocapacitive effects, while the maintained symmetry across scan rates indicates excellent reversibility of the charge storage process (Kashif *et al.* 2024a). Overall, these results strongly support the positive impact of cobalt doping on the electrochemical performance of praseodymium, making it a promising material for high-performance supercapacitor applications.

The galvanostatic charge-discharge (GCD) curves presented for pure praseodymium oxide and cobalt-doped praseodymium oxide (Fig. 11) illustrate the electrochemical performance of these materials for supercapacitor applications. In the case of pure praseodymium oxide, the charge-discharge times are relatively short, with discharge durations of approximately 70 seconds at 1 V, 80 seconds at 2 V, and 90 seconds at 3 V, indicating a limited energy storage capacity. The calculated specific capacitance values for pure praseodymium oxide are around 175 F/g at 1 V, 190 F/g at 2 V, and 210 F/g at 3 V, suggesting moderate capacitive behavior but suboptimal charge retention. This could be attributed to low electrical conductivity and a lack of redox-active sites, which limits charge storage efficiency. Cobalt-doped praseodymium oxide exhibits

significantly extended charge-discharge durations, demonstrating a remarkable improvement in supercapacitive performance. The discharge times for the doped material reach approximately 400 seconds at 1 V, 450 seconds at 2 V, and over 600 seconds at 3 V, which directly correlates with an enhanced charge storage capacity. The corresponding specific capacitance values increase significantly to approximately 270 F/g at 1 V, 386 F/g at 2 V, and 599 F/g at 3 V, indicating a substantial improvement compared to pure praseodymium oxide. This enhancement can be attributed to the presence of cobalt, which likely increases electrical conductivity, provides additional redox-active sites, and improves ion diffusion kinetics, ultimately leading to superior charge retention and higher capacitance (Czagany *et al.* 2024; Jadhav *et al.* 2023; Xu *et al.* 2021).

Table 4. Comparison studies of previous works

Material	Synthesis Method	Specific Capacitance (F/g)	Scan Rate (mV/s)	Energy Density (Wh/kg)	Power Density (kW/kg)
Ag-doped Co_3O_4	Chemical Synthesis	470	5	25.2	4.3
Mn-doped Co_3O_4	Hydrothermal	380	10	17.4	3.1
Ni-Co Layered Double hydroxide	Electrodeposition	450	5	22.1	3.9
Fe-doped Co_3O_4	Solvothermal	420	10	20.5	3.4
Cobalt Manganese oxide	Solid-State	375	5	16.8	3.0
MoS_2/ Co_3O_4Composite	Hydrothermal	460	10	24.0	4.1
$LaCoO_3$ Nanoflakes	Hydrothermal	410	10	19.8	3.2
Ce-doped Co_3O_4Nanoflakes	Hydrothermal	350	10	15.6	3.0
$CoFe_2O_4$/Graphene/ Polyaniline	Sol-Gel	495	10	26.0	4.5
Cobalt-doped praseodymium oxide (Present Work)	Sol-Gel	**599**	10	**27.5**	**4.9**

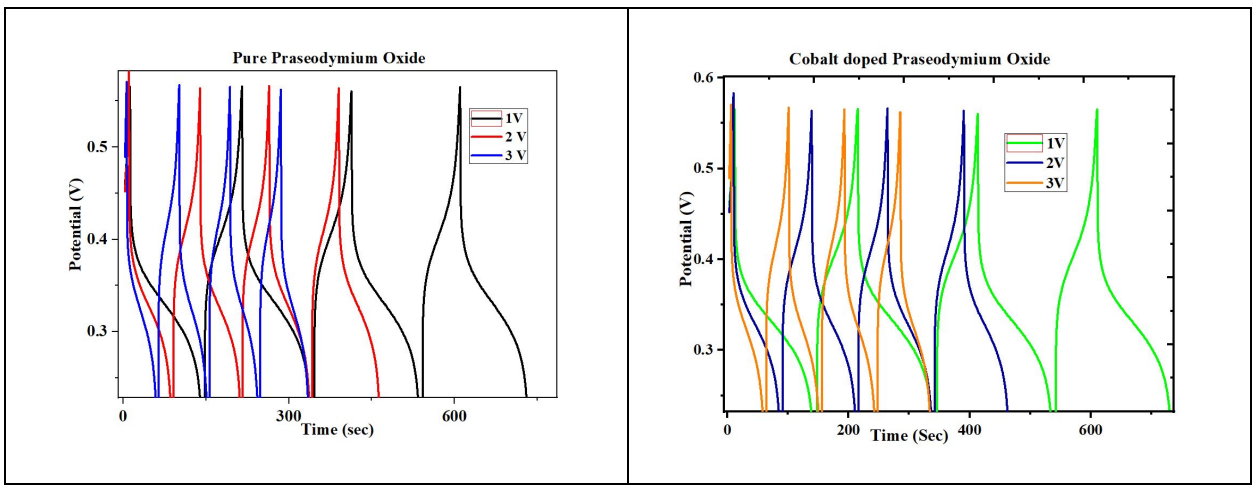


Fig. 11: GCD studies of pure praseodymium oxide and cobalt-doped praseodymium oxide

3.8 Galvanostatic Charge Discharge

The comparison between the two materials clearly demonstrates that cobalt doping significantly enhances the electrochemical performance of praseodymium oxide, making it a much more effective electrode material for high-performance supercapacitors. The prolonged discharge times, higher capacitance, and improved charge retention suggest that cobalt-doped praseodymium oxide could be a promising candidate for next-generation energy storage devices.

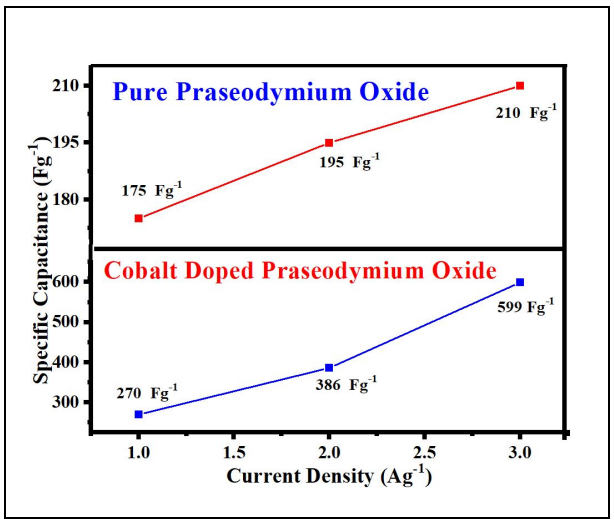


Fig. 12: Specific capacitance calculation

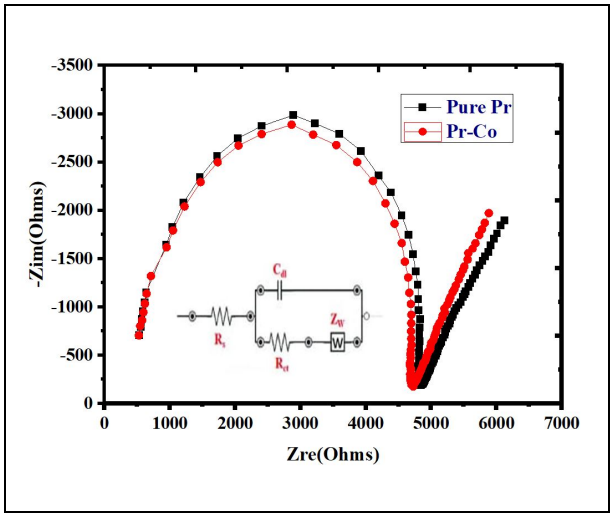


Fig. 13: EIS analysis of pure Pr oxide and Co-doped Pr oxide

The comparison between pure praseodymium oxide and cobalt-doped praseodymium oxide clearly demonstrates that Co-doped praseodymium oxide (Fig. 12) is superior material for supercapacitor applications. The specific capacitance of cobalt-doped praseodymium oxide is significantly higher, increasing from 270 F/g at 1 A/g to 599 F/g at 3 A/g, whereas pure Pr exhibits a much lower capacitance range of 175 F/g to 210 F/g under the same conditions. This substantial enhancement in capacitance can be attributed to the improved electrical conductivity and additional electroactive sites introduced by cobalt doping, which facilitate better charge transfer kinetics and efficient ion diffusion. Furthermore, cobalt-doped praseodymium oxide exhibits excellent rate capability, as indicated by its steep increase in capacitance with rising current density, making it highly suitable for high-power applications requiring rapid charge-discharge cycles (Yang *et al.* 2022). In contrast, the slower capacitance increase in pure Pr suggests higher internal resistance and limited charge storage efficiency, restricting its effectiveness as a supercapacitor electrode. Overall, the superior electrochemical performance, enhanced charge storage capacity, and better conductivity of cobalt-doped praseodymium oxide make it the optimal choice for innovative supercapacitors, ensuring both high energy density and power capability for advanced energy storage applications (Wang *et al.* 2011; Hussain *et al.* 2024b; Hussain *et al.* 2024c).

3.9 Electrochemical Impedance Spectroscopy

The Nyquist plot analysis provides valuable insights into the electrochemical characteristics of pure Pr and cobalt-doped praseodymium oxide perovskite materials (Fig. 13) for supercapacitor applications. The results demonstrate that both materials exhibit favorable charge transfer and ion diffusion properties, with cobalt-doped praseodymium oxide showing slightly enhanced performance. The smaller semicircle diameter in the cobalt-doped praseodymium oxide sample indicates reduced charge transfer resistance, suggesting better electronic conductivity and faster charge-discharge capabilities compared to pure Pr_6O_{11}. This improvement can be attributed to the synergistic effect between praseodymium and cobalt atoms, creating additional active sites for charge storage and transfer. The well-defined transition from the semicircular region to the linear Warburg portion indicates efficient double-layer capacitance formation and good ion diffusion characteristics, essential for high-performance supercapacitors (Zeshan *et al.* 2025). The similar impedance patterns between both materials, coupled with the relatively small solution resistance, suggest that incorporating cobalt maintains the fundamental charge storage mechanisms while potentially offering cost advantages. These characteristics make these materials particularly suitable for applications requiring rapid energy storage and release, such as in electric vehicles or grid energy storage systems, where high power density, fast charge-discharge rates, and long-term stability are crucial. The improved electrochemical performance of cobalt-doped praseodymium oxide, combined with the cost benefits of using less praseodymium, presents a promising direction for developing more efficient and economically viable supercapacitor materials (Kashif *et al.* 2024b; Seliem *et al.* 2024b).

4. CONCLUSION

Cobalt-doped praseodymium oxide was successfully synthesized *via* the sol-gel method, demonstrating substantial improvements in physicochemical and electrochemical properties compared to pure praseodymium oxide. The incorporation of cobalt enabled better control over particle size (~20.65 nm) and morphology, as evidenced by SEM, with EDX analysis confirming uniform elemental distribution. Surface area (BET) increased

significantly from 5.198 m^2/g to 9.297 m^2/g, enhancing electrolyte accessibility and ion diffusion, although with reduced pore volume. Structural and compositional characterization using FTIR and XPS confirmed metal–oxygen bonding and the presence of Pr^{3+}, mixed Co^{2+}/Co^{3+} states, and abundant oxygen vacancies, all of which are conducive to enhanced redox behavior. The Co 2p peaks (~780.1 eV and ~795.3 eV) with satellites, and O 1s peaks (~528.6 eV and ~531.2 eV), indicate improved defect chemistry and active redox centers due to cobalt doping. Electrochemical testing revealed that cobalt-doped praseodymium oxide achieved a high specific capacitance (599 F/g at 3 A/g) with excellent rate performance. The device also exhibited an energy density of 27.5 Wh/kg and a power density of 4.9 kW/kg, underscoring its potential for high-performance supercapacitor applications. Overall, cobalt doping plays an important role in enhancing the surface area, oxygen vacancy concentration, and electrochemical activity of praseodymium oxide, thereby making $Pr_{1-x}Co_xO_3$ a promising electrode material for next-generation energy storage devices.

ACKNOWLEDGEMENTS

The corresponding author, Dr. V. Saraswathi, is grateful to the National College Instrument facility, National College (Autonomous), Tiruchirappalli, Tamil Nadu, India for providing lab facility.

FUNDING

This research did not receive any specific grant from funding agencies in the public, commercial, or not for profit sectors.

AUTHOR CONTRIBUTIONS

A. Cathirin Preethi took part in investigation, methodology, data collection, writing-original draft, and writing-review & editing. Dr. V. Hariharakrishnan: Supervision, writing-review, editing, methodology, and conceptualization. Dr. V. Saraswathi: Supervision writing-review and editing. Dr. D. Saravanan: Supervision and editing. Dr. S. Meiyazhagan: Characterization.

COPYRIGHT

This article is an open-access article distributed under the terms and conditions of the Creative Commons Attribution (CC BY) license (http://creativecommons.org/licenses/by/4.0/).

CONFLICT OF INTEREST

The authors declare that there is no competing and conflict of interest in this research article.

REFERENCES

Alenad, A. M., Ahmad, N., Aman, S., Saeed, M. N., Farid, H. M. T. and Taha, T. A. M., Engineering of the crystalline state towards a defective state of CeCoO 3 perovskite for the OER process in alkaline medium, *J. Taibah Univ. Sci.,* 17(1), 2231132 (2023). https://doi.org/10.1080/16583655.2023.2231132

Alenad, A. M., Aman, S., Ahmad, N., Rashid, A. R., Abid, A. G., Manzoor, S., Nisa, M. U., Messali, M., Alzahrani, H. A. and Taha, T. A. M., Facile synthesis of SmSe2 over multiwalled carbon nanotubes for efficient water-splitting applications, *J. Korean Ceram. Soc*., 61(1), 44–54 (2024). https://doi.org/10.1007/s43207-023-00328-y

Ali, F., Khalid, N. R., Nabi, G., Hamid, U. A. and Ikram, M., Hydrothermal synthesis of cerium-doped Co_3O_4 nanoflakes as electrode for supercapacitor application, *Int. J. Energy Res.,* 45(2), 1999–2010 (2020). https://doi.org/10.1002/er.5893

Alshammari, D. A., Ahmed, I. A., Alahmari, S. D., Abdullah, M., Aman, S., Ahmad, N., Henaish, A M. A., Ahmad, Z., Farid, H. M. T. and Bahy, -E. Z. M., Electrochemical investigation of niobium doped nickel selenide nanostructure for supercapacitor devices, *J. Energy Storage*, 75, 109886 (2024). https://doi.org/10.1016/j.est.2023.109886

Althubiti, N. A., Hassan, M. M., Waheed, M. S., Aman, S., Khosa, R. Y., Farid, H. M. T., Nazir, A., Ansari, M. Z., Abdulaziz, F. and Taha, T. A. M., Fabrication of novel zinc selenide/cadmium oxide nanohybrid electrode via hydrothermal route for energy storage application, *J. Energy Storage*, 70, 108154 (2023). https://doi.org/10.1016/j.est.2023.108154

Aman, S., Alahmari, S. D., Khan, S. A., Sehemi, -A. A. G., Ejaz, S. R., Ahmad, N., Alharbi, F. F., Sadaf, A. and Farid, H. M. T., Hydrothermal development of bimetallic sulfide nanostructures as an electrode material for supercapacitor application, *Energy Fuels*, 37(22), 17473–17483 (2023). https://doi.org/10.1021/acs.energyfuels.3c03380

BaQais, A., Amin, M. A., Aman, S., Ejaz, S. R., Farid, H. M. T. and Bahy, E. Z. M., Tailoring of electrochemical properties on Nd-doped Ni3S2 electrode via doping strategy for supercapacitor application, *Electrochim. Acta*, 467, 143070 (2023). https://doi.org/10.1016/j.electacta.2023.143070

Czagany, M., Hompoth, S., Keshri, A. K., Pandit, N., Galambos, I., Gacsi, Z. and Baumli, P., Supercapacitors: an efficient way for energy storage application, *Mater*., 17(3), 702 (2024). https://doi.org/10.3390/ma17030702

De, A., Kim, M. S., Adhikari, A., Patel, R. and Kundu, S., Sol–gel-derived nanostructured electrocatalysts for oxygen evolution reaction: a review, *J. Mater. Chem. A,* 12(31), 19720–19756 (2024). https://doi.org/10.1039/d4ta01442a

Ejaz, Y., Alotaibi, B. M., Alrowaily, A. W., Alyousef, H. A., Somaily, H. H. and Aman, S., Development of cost-efficient BaMnO3/rGO nanocomposite as electrode for energy storage applications in supercapacitor, *Ceram. Int.,* 50(15), 27508–27519 (2024). https://doi.org/10.1016/j.ceramint.2024.05.050

Gao, C., Zhu, J., Ye, S., Li, M., Wang, H. and He, J., Novel high-entropy perovskite titanate: A potential thermal protective material with improved thermophysical properties, *J. Eur. Ceram. Soc*., 45(2), 116878 (2025). https://doi.org/10.1016/j.jeurceramsoc.2024.116878

Gao, H. and Wang, B., A first-principles study on structural stability and magnetoelectric coupling of two-dimensional BaTiO3 ultrathin film with Cr and Cu substituting Ti site, *APL Mater.,* 12(9), 091117 (2024). https://doi.org/10.1063/5.0223008

Gouadria, S., Abdullah, M., Alharbi, F. F., Aman, S. and Farid, H. M. T., Determination of doping strategy on the electrochemical performance of the hydrothermally prepared perovskite material, *J. Sol-Gel Sci. Technol.,* 113, 617-626 (2025). https://doi.org/10.1007/s10971-024-06638-9

Hussain, M., Alanazi, M. M., Abdelmohsen, S. A. M., Abdullah, M., Ali, M., Aman, S., Sehemi, -A. A. G., Henaish, A. M. A. and Farid, H. M. T., Enhanced Supercapacitive Performance of FeAl2O4 Nanoparticles with Neodymium (Nd) Doping by Sonication Method, *JOM,* 76(6), 3185–3194 (2024a). https://doi.org/10.1007/s11837-024-06518-1

Hussain, M., Alotaibi, B. M., Alrowaily, A. W., Alyousef, H. A., Alotiby, M. F., Abdullah, M., Sehemi, -A. A. G., Henaish, A. M. A., Ahmad, Z. and Aman, S., Synthesis of high-performance supercapacitor electrode materials by hydrothermal route based on ZnSe/MnSe composite, *J. Phys. Chem. Solids,* 188, 111919 (2024b). https://doi.org/10.1016/j.jpcs.2024.111919

Hussain, M., Maati, L. A. E., Alomar, M. A., Ali, M., Abdullah, M., Aman, S. and Farid, H. M. T., Enhancement of capacitive properties of CE-Doped MNAL2O4 electrode for high performance energy storage application s, *JOM,* 76(8), 4587–4597 (2024c). https://doi.org/10.1007/s11837-024-06563-w

Jadhav, S., Kalubarme, R., Chauhan, R., Singh, A., Kale, B., Ashokkumar, M. and Gosavi, S., Nanocrystalline Ag-doped cobalt oxide as a flexible electrode material for high performance supercapacitor application, *J. Energy Storage*, 58, 106326 (2023). https://doi.org/10.1016/j.est.2022.106326

Jiang, L., Shi, H., Han, M., Zhang, Y., Liang, J., Chen, J., Geng, S., Tong, L. and Sheng, L., Rearrangement of pore Structure-Enabled Micropore-Dominant N,O Co-Doped carbon for ultrafast Charge/Discharge rate supercapacitors at Commercial-Scale mass loading, *ACS Sustainable Chem. Eng*., 12(51), 18422-18433 (2024). https://doi.org/10.1021/acssuschemeng.4c07871

Kashif, M., Khan, S., Wajahat, H., Alharbi, F. F., Sehemi, -A. A. G., Aman, S. and Alqurashi, H., Physicochemical and electrochemical investigation of lead sulphide-graphene oxide hybrid nanostructure for energy storage applications, *J. Electroanal. Chem*., 974, 118680 (2024a). https://doi.org/10.1016/j.jelechem.2024.118680

Kashif, M., Khan, S., Wajahat, H., Alharbi, F. F., Sehemi, -A. A. G., Aman, S. and Alqurashi, H., Physicochemical and electrochemical investigation of lead sulphide-graphene oxide hybrid nanostructure for energy storage applications, *J. Electroanal. Chem*., 974, 118680 (2024b). https://doi.org/10.1016/j.jelechem.2024.118680

Lakal, N., Dubal, S. and Lokhande, P. E., Supercapacitors: An introduction, *Nanotechnol. Automot. Ind. Micro Nano Technol.,* 459–466 (2022). https://doi.org/10.1016/b978-0-323-90524-4.00022-0

Lakshmi, K. C. S. and Vedhanarayanan, B., High-Performance Supercapacitors: A Comprehensive review on paradigm shift of conventional energy storage devices, *Batteries*, 9(4), 202 (2023). https://doi.org/10.3390/batteries9040202

Lokhande, P. E., Jagtap, C., Kadam, V., Udayabhaskar, R., Shaikh, S. F., Ali, R. and Pathan, H. M., Synergistic electrochemical behaviour of hydrothermally deposited Ni·Co LDH/rGO nanocomposite on nickel foam, *J. Energy Storage*, 97, 112910 (2024). https://doi.org/10.1016/j.est.2024.112910

Mahato, S. S., Mahata, D., Panda, S., & Mahata, S., Perspective Chapter: Sol-Gel Science and Technology in context of Nanomaterials – Recent Advances, *IntechOpen eBooks,* (2023). https://doi.org/10.5772/intechopen.111378

Manzoor, S., Alsaiari, N. S., Katubi, K. M., Nisa, M. U., Abid, A. G., Chughtai, A. H., Abdullah, M., Aman, S., Buriahi, -A. M. S. and Ashiq, M. N., Facile fabrication of SnSe nanorods embedded in GO nanosheet for robust oxygen evolution reaction, *J. Taibah Univ. Sci.*, 17(1), 2151298 (2023). https://doi.org/10.1080/16583655.2022.2151298

Matović, B., Pantić, J., Prekajski, M., Stanković, N., Bučevac, D., Minović, T. and Čebela, M., Synthesis and characterization of Pr6O11 nanopowders, *Ceram. Int.,* 39(3), 3151–3155 (2013). https://doi.org/10.1016/j.ceramint.2012.09.098

Moorthi, K., Sivakumar, B., Chokkiah, B., Valdes, H. and Mohan, S., Morphological impact of Perovskite-Structured lanthanum cobalt oxide (LACOO3) nanoflakes toward supercapacitor applications, *ACS Appl. Nano Mater.,* 7(16), 18511–18522 (2024). https://doi.org/10.1021/acsanm.3c05803

Naeem, S., Electrodeposited Cobalt Hydroxide Thin Films: A Comprehensive Investigation from Synthesis to Advanced Electrochemical Behavior for High-Performance Energy Storage, *Trans. Electr. Electron. Mater.,* 25(5), 589–599 (2024a). https://doi.org/10.1007/s42341-024-00542-3

Naeem, S., Patil, A. V., Shaikh, A. V., Shinde, U. P., Husain, D., Alam, M. T., Sharma, M., Tewari, K., Ahmad, S., Shah, A. A., Ali, S. A. and Ahmad, A., A review of Cobalt-Based metal hydroxide electrode for applications in supercapacitors, *Adv. Mater. Sci. Eng.*, 2023(1), 1133559 (2023a). https://doi.org/10.1155/2023/1133559

Naeem, S., Shaikh, A. V., Shinde, U. P. and Patil, A. V., Electrochemical deposition, synthesis, and characterization of Dopant-Free cobalt hydroxide as an enhanced electrode material for supercapacitors, *ES Energy Environ.,* 21, 915(2023b). https://www.espublisher.com/journals/articledetails/915/

Naeem, S., Shaikh, A., Rasool, A., Husain, D., Alam, M. T. and Patil, A., Enhancing supercapacitor performance through electrodeposition of cobalt hydroxide thin film: structural analysis, morphological characterization, and investigation of electrochemical properties, *Ionics*, 30(1), 399–405 (2024b). https://doi.org/10.1007/s11581-023-05293-4

Naeem, S., Shinde, U. and Patil, A., Cobalt hydroxide-based electrodes for supercapacitors: Synthesis, characterization, and electrochemical performance optimization, *Energy Storage*, 6(1), e516 (2023c). https://doi.org/10.1002/est2.516

Naeem, S., Electrodeposited Cobalt Hydroxide Thin Films: A Comprehensive Investigation from Synthesis to Advanced Electrochemical Behavior for High-Performance Energy Storage, *Trans. Electr. Electron. Mater.,* 25(5), 589–599 (2024c). https://doi.org/10.1007/s42341-024-00542-3

Naeem, S., Patil, A. V., Shaikh, A. V., Shinde, U. P., Husain, D., Alam, M. T., Sharma, M., Tewari, K., Ahmad, S., Shah, A. A., Ali, S. A. and Ahmad, A., A review of Cobalt-Based metal hydroxide electrode for applications in supercapacitors, *Adv. Mater. Sci. Eng.*, 2023(1), 1133559 (2023d). https://doi.org/10.1155/2023/1133559

Olabi, A. G., Abbas, Q., Makky, A. A. and Abdelkareem, M. A., Supercapacitors as next generation energy storage devices: Properties and applications, *Energy*, 248, 123617 (2022). https://doi.org/10.1016/j.energy.2022.123617

Pardeshi, O. M., Naeem, S. and Patil, A. V., Synthesis of $FeVO_4$ nanoparticles using sol-gel auto-combustion method and their application in supercapacitors, *Energy Storage*, 6(5), e683 (2024). https://doi.org/10.1002/est2.683

Saha, P., Nath, N. C. D., Islam, M. M., Aziz, M. A. and Ahammad, A. J. S., Recent progress of High-Energy Density supercapacitors based on nanostructured nickel oxides, *Electrochim. Acta*, 504, 144892 (2024). https://doi.org/10.1016/j.electacta.2024.144892

Seliem, A. F., Mohammed, A. Y. A., Attia, A., Ahmad, N., Aman, S. and Ibrahim, M. M., Development of NB-Doped $BIFEO_3$ via hydrothermal method for photocatalytic degradation of rhodamine B (RHB) dye, *JOM*, 76(1), 408–417 (2024a). https://doi.org/10.1007/s11837-023-06225-3

Seliem, A. F., Mohammed, A. Y. A., Attia, A., Aman, S., Ahmad, N. and Ibrahim, M. M., ZIF-67 MOF-Derived MN3O4 @ N-Doped C as a supercapacitor electrode in different alkaline media, *ACS Omega*, 9(15), 17563-17576 (2024b). https://doi.org/10.1021/acsomega.4c00676

Tian, Y., Cai, Y., Chen, Y., Jia, M., Hu, H., Xie, W., Li, D., Song, H., Guo, S. and Zhang, X., Accessing the O Vacancy with Anionic Redox Chemistry Toward Superior Electrochemical Performance in O3 type Na-Ion Oxide Cathode, *Adv. Funct. Mater*., 34(32), 2316342 (2024). https://doi.org/10.1002/adfm.202316342

Wang, X., Yang, C., Wang, T. and Liu, P., Praseodymium oxide/polypyrrole nanocomposites for electrochemical energy storage, *Electrochim. Acta*, 58, 193–202 (2011). https://doi.org/10.1016/j.electacta.2011.09.060

Wei, Y., Sun, X., Meng, X., Li, Z., Zhang, L., Zhou, K. and Ma, Z., Enhancing the properties of Cd-free MgZnS buffer for solar cells by co-sputtering ZnS and Mg targets, *Mater. Today Commun*., 39, 108766 (2024). https://doi.org/10.1016/j.mtcomm.2024.108766

Xu, J. M., Yan, A. L., Wang, X. C., Wang, B. Q. and Cheng, J. P., A review of cobalt monoxide and its composites for supercapacitors, *Ceram. Int*., 47(16), 22229–22239 (2021). https://doi.org/10.1016/j.ceramint.2021.04.262

Xu, X., Dong, Y., Hu, Q., Si, N. and Zhang, C., Electrochemical hydrogen Storage Materials: State-of-the-Art and Future Perspective, *Energy Fuels*, 38(9), 7579–7613 (2024). https://doi.org/10.1021/acs.energyfuels.3c05138

Yadlapalli, R. T., Alla, R. R., Kandipati, R. and Kotapati, A., Super capacitors for energy storage: Progress, applications and challenges, *J. Energy Storage*, 49, 104194 (2022). https://doi.org/10.1016/j.est.2022.104194

Yang, L., Zhu, Q., Yang, K., Xu, X., Huang, J., Chen, H. and Wang, H., A review on the application of Cobalt-Based nanomaterials in supercapacitors, *Nanomater.,* 12(22), 4065 (2022). https://doi.org/10.3390/nano12224065

Zahra, T., Alotaibi, B. M., Alrowaily, A. W., Alyousef, H. A., Aman, S., Hussein, K. I. and Karim, M. R., Fabrication of enhanced electrochemical AlBiO3/g-CN nanocomposite electrode material via hydrothermal approach for supercapacitor applications, *Diamond Relat. Mater*., 148, 111355 (2024a). https://doi.org/10.1016/j.diamond.2024.111355

Zahra, T., Alotaibi, B. M., Alrowaily, A. W., Alyousef, H. A., Sehemi, A. A. G. and Aman, S., Boosting the energy-storing performance of hydrothermally synthesized ZnO by MnTe for supercapacitor applications, *J. Mater. Sci. Mater. Electron.,* 35(16), 1086 (2024b). https://doi.org/10.1007/s10854-024-12807-x

Zeshan, M., Eman, S., Fallatah, A. M., Ibrahim, M. M., Almalki, A. S., Aslam, M. and Bahy, E. Z. M., Facile fabrication of binary metal chalcogenides (MS@NS) for supercapacitors applications via hydrothermal route, *J. Sol-Gel Sci. Technol.,* 113, 855-867 (2025) https://doi.org/10.1007/s10971-025-06665-0

Zeshan, M., Gassoumi, A., Alsalhi, S. A., Alahmari, S. D., Ahmed, K. and Eman, S., Fabrication of ZnCr2O4/MnO2 composite electrodes by Sol gel Synthesis for Advanced Symmetric Supercapacitors, *Ceram. Int.*, 50(22), 47585-47594 (2024). https://doi.org/10.1016/j.ceramint.2024.09.104